J Mater Sci (2009) 44:4270–4278
DOI 10.1007/s10853-009-3624-3

Free-volume properties and toughening behavior of cyanate ester resin/carboxyl-randomized liquid butadiene-acrylonitrile rubber composites

**Minfeng Zeng · Xudong Sun · Xiandong Yao ·
Yun Wang · Mingzhu Zhang · Baoyi Wang ·
Chenze Qi**

Received: 19 March 2009 / Accepted: 19 May 2009 / Published online: 5 June 2009

Abstract The toughness of cyanate ester resin (CE) matrix was improved significantly with addition of carboxyl-randomized liquid butadiene-acrylonitrile rubber (CRBN). The curing behavior of the system was studied by differential scanning calorimetric (DSC) and Fourier transform infrared spectrum (FTIR). The results showed that carboxyl groups on the CRBN chain had slight activation effect to CE curing reaction at the beginning of the cure process. Phase separation was the main toughening mechanism for CE/CRBN composites. The existence of micro-size pores induced by small amount of the low weight molecular part of CRBN might be another toughening mechanism. The toughening mechanism was proved powerfully from the aspect of free-volume using positron annihilation lifetime spectroscopy (PALS). PALS is qualitatively sensitive to the existence of pores induced by low molecular weight part of CRBN during curing process.

Introduction

Cyanate ester (CE) resin is one of the most important kinds of thermosetting resins and has received more and more attentions for its superior mechanical properties, low water absorptivity, low outgassing in curing, high environment resistance, and excellent dielectric properties. It has been widely used as adhesives and matrixes for composites. However, like most other thermosetting resins, it has the drawback of brittleness. A number of studies have been carried out to improve the toughness of cyanate resins, such as the preparation of flexibilized cyanate resins, the incorporation of monocyanates, the utilization of rubber-toughening technologies, the use of organoclay toughening, and the preparation of semi-interpenetrating networks have been proven useful [1, 2]. Among them, using carboxyl-terminated butadiene-acrylonitrile rubber (CTBN) and other similarly functionalized liquid nitrile rubbers were proven to be one of the most successful techniques [3–8]. Usually, during the curing reaction of thermosetting resin/rubber systems, the rubber phase would separate and form tiny particles that dispersed in the thermosetting resin network after curing. Recently, Feng et al. [9, 10] reported their works on the mechanism of the toughening behavior of CTBN on CE. According to the reported results, there are two toughening mechanisms. Phase separation and pores toughening mechanism function together to improve the toughness of the CE/CTBN system. The gas molecules (the decomposition products of low molecular weight part of CTBN (about 3%)) were trapped by the crosslinking network of CE and formed the pores after the curing process [9–11].

Positron annihilation lifetime spectroscopy (PALS) has been used as a unique technique to probe nano-scale voids and the free-volume properties of polymers for many years [12–15]. The positron, e^+, is the anti-particle of the electron which annihilates by combining with an electron, e^-, to generate photons of a specific energy. Positrons are generated by the decay of certain unstable isotopes, one of the most commonly used being $^{22}_{11}Na$ which decays to $^{22}_{10}Ne$

M. Zeng (✉) · X. Sun · X. Yao · Y. Wang · M. Zhang · C. Qi
Institute of Applied Chemistry, Shaoxing University, Shaoxing
312000, People's Republic of China
e-mail: Zengmf@zscas.edu.cn

C. Qi
e-mail: Qichenze@zscas.edu.cn

B. Wang
Institute of High Energy Physics, The Chinese Academy
of Science, Beijing 100049, People's Republic of China

with the simultaneous emission of e^+ and a γ-ray of 1.28 MeV. The positrons emitted have a distribution energies between zero and 540 keV and are thermalized by inelastic collisions with the surrounding media. The thermalization process will cause ionization of the media with production of secondary electrons, which can form a bound positron–electron pair, Positronium (Ps). There are two kinds of Ps atoms. The para-positronium (*p*-Ps), in which the spins of the positron and electron are antiparallel, has a lifetime of 0.125 ns by self-annihilation in vacuum; while the ortho-positronium (*o*-Ps), in which the spins of the positron and electron are parallel, has a longer lifetime of 142 ns in vacuum. In molecular solids three annihilation processes are possible: free positron, *o*-Ps and *p*-Ps annihilation. Free positrons have a lifetime of about 0.4 ns through interaction with the outer electrons of molecules with which they collide. *o*-Ps atoms are preferentially localized in atom-scale holes and their lifetime is shortened to about 1–5 ns by a spin exchange or pick-off annihilation with other electrons from surrounding molecules. The *o*-Ps lifetime, τ_3 directly correlates with the size of free-volume holes and its intensity, I_3 contains information about the free-volume concentration. The average radius (R) of free-volume holes on a quantum mechanical model developed by Tao [16] was proposed as the following equation:

$$\frac{1}{\tau_3} = 2\left\{1 - \frac{R}{R+\Delta R} + \frac{1}{2\pi}\sin\left(\frac{2\pi R}{R+\Delta R}\right)\right\} \tag{1}$$

where R is the radius of the free-volume hole, ΔR (=0.1656 nm) is derived from fitting the observed *o*-Ps lifetimes in molecular solids with known hole sizes [17]. Furthermore, the fractional free-volume f is valuated in terms of the *o*-Ps intensity I_3 and the size of free-volume hole ($V = 4\pi R^3/3$):

$$f = CVI_3 \tag{2}$$

where C is a constant. Usually, we use apparent free-volume fraction, f_{app}:

$$f_{\mathrm{app}} = VI_3 \tag{3}$$

because what we concern is not the absolute value of free-volume fraction, but instead the variation of free-volume fraction. A study on the behavior of free-volume in the two-component blends will help us to understand the interaction between the different macromolecular chains and the relationship between the microstructure and the properties of blends. Our recent works [18–20] have showed that PALS is an effective tool to probe the atomic-scale microstructure of thermosetting/liquid rubber composites. It has been confirmed that the PALS is still valid in CE/CTBN system where macro-pores are filled with gas molecules [20].

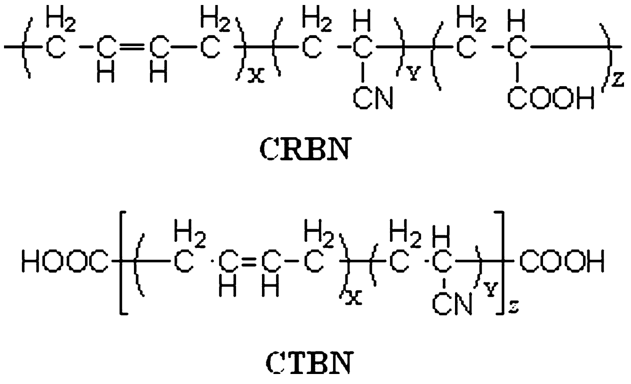

Fig. 1 The molecular structure of CRBN and CTBN

In the present study, a new kind of butadiene-acrylonitrile rubber (i.e., carboxyl-randomized liquid butadiene-acrylonitrile rubber (CRBN)) has been used to modify the CE network. As shown in Fig. 1, the carboxyl groups of CRBN are on the rubber backbone instead of the end compared with CTBN. CRBN might be more compatible with CE than CTBN because it can supply more active hydrogen that is able to catalyze the curing process applied to the system. The PALS has been used to investigate the changes of the free-volume properties in CE/CRBN system with different contents of CRBN. The purpose of the present study is to evaluate the toughening effect of the CRBN for CE and then discuss the toughening mechanism from the aspect of free-volume.

Experiments

Materials

A phenolic-based CE resin (melting point: 76 °C) was supplied by Jinan Special Structure Institute of China Aero-Industry (Jinan, China). The CRBN and CTBN were provided by Lanzhou Chemical Industry Company (Lanzhou, China). The molecular weight of CRBN was between 3000 and 5000. The acrylonitrile content of the used CRBN was 22–25 wt%. The molecular weight of CTBN was between 2000 and 3000. The acrylonitrile content of the used CTBN was 25% by weight. Mold release agent (JR105 silicone grease) was provided by Jinrong Grease Company (Fuyang, China).

Preparation of the composites

CE was placed in a beaker maintained at 90 °C. Certain amount of CRBN (rubber content: 0, 3, 5, 8, 10, 15% by weight) was added to the CE resin at 90 °C with stirring.

After completely mixing, mixture was quickly poured into a preheated steel mold coated with right amounts of the mold release agent (just put a cover over the steel mold). After degasification under vacuum (about 1000 Pa) for 30 min at 110 °C, the cure procedure for the samples was as follows (at normal pressure): 130 °C/1 h + 150 °C/1 h + 170 °C/1 h + 190 °C/1 h + 210 °C/1 h + 230 °C/1 h + 250 °C/1 h to form the specimens. Then the samples were cooled down naturally.

Characterization of the composites

The unnotched impact strength was measured with a Charpy impact tester (XCJ-5, Chengde Testing Machine Co. Ltd., China). The tests were according to the Chinese national standard methods for impact resistance of resin casting body (GB/T 2571-1995) at 23 ± 2 °C. The tensile properties were measured with a universal materials testing machine (SANS Testing Machine Co. Ltd., Shenzheng, China) with a crosshead speed of 2 mm/min. The tensile measurements were according to the Chinese national standard methods for tensile properties of resin casting body (GB/T 2568-1995) at 23 ± 2 °C. Five specimens of each group were prepared and tested.

The reactions were tracked by infrared spectrometry with Fourier transform infrared spectrum (FTIR-Nicolet 740). The pre-polymer of CE-CRBN was blended with appropriate amount of KBr to form a sheet. The sheet was scanned firstly by FTIR for its initial curve, and then the sheet was placed in an oven at 170 °C for certain time interval (10, 20, 30, 60, 90, and 120 min) and scanned by FTIR for its part-cured curve.

Differential scanning calorimetric (DSC, PekinElmer DSC-7) measurements were made at a scan rate of 10 °C/min with 4–6 mg samples in a nitrogen atmosphere.

The morphology of the composites was examined by JEM-6360 scanning electron microscopy (SEM). All the samples were coated with gold to improve SEM imaging. In order to view phase separated rubber particles with a transmission electron microscope (TEM), the ultra thin sample films were treated firstly by osmium tetraoxide (OsO_4) and then observed with a JEM-1200EX TEM.

Thermo gravimetric analysis (TGA) was performed using a Mettler-Toledo TGA/SDTA851e (Mettler-Toledo International Inc.) thermal analyzer. The samples were heated from 30 to 250 °C at a heating rate of 5 °C/min under nitrogen atmosphere.

PALS measurement

Positron annihilation lifetime spectroscopy (PALS) was measured with an EG&G ORTEC fast-fast lifetime spectrometer (ORTEC Co., Tennessee, USA) with a FWHM = 190 ps for a ^{60}Co prompt peak of 1.18 and 1.33 MeV γ rays. A 6×10^5 Bq of positron source (^{22}Na) was deposited between two Kapton films (3 μm in thickness), which was sandwiched between two identical composite samples. All PALS measurements were performed at room temperature. Every spectrum contained about 10^6 counts. The resulting spectra were consistently modeled with a three-component fit with the computer program PATFIT.

Results and discussion

Curing behavior of the system

The cyclotrimerization reaction is the dominant reaction pathway during the cure of cyanate-based resins to form highly crosslinked polytriazine networks [21, 22]. The reaction can be catalyzed by coordination of metal catalysts and an active hydrogen initiator or thermally induced at a temperature higher than 190 °C. Figure 2 shows the DSC results of the curing reaction of the composites. The addition of CRBN relaxed the curing reaction of CE, and the CE/CRBN system shows a broad and moderate curing peak compared to pure CE system. The onset temperature of CE curing shows a slight decrease with the addition of CRBN. This means that carboxyl groups on the CRBN chain have a slight activation effect on the CE curing reaction at the beginning of the curing process. The reason is that the carboxyl groups on the CRBN molecule chain supplies active hydrogen to the system. Thus, the onset temperature of the cure process of the system decreases with the addition of CRBN. The onset temperature of the cure process of CE/CRBN system is lower than CE/CTBN system [20]. CRBN is more compatible with CE than CTBN because it can supply more active hydrogen. As seen in Fig. 2, both the end temperature and the peak temperature of CE curing show a slight increase with addition of CRBN. This can be attributed to the steric

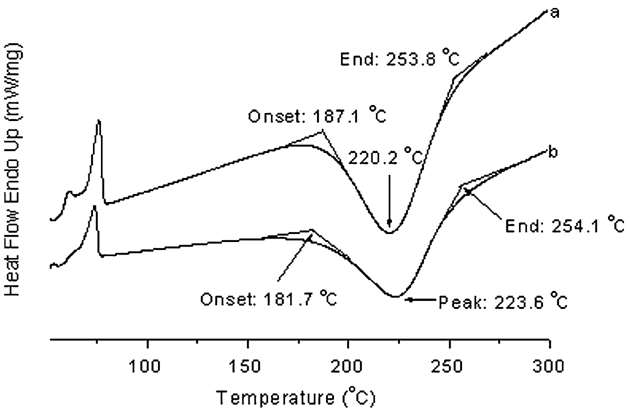

Fig. 2 DSC curves of CE (a) and CE/CRBN (CRBN 8%) (b)

effect during the curing reaction of CE. The addition of CRBN would decrease the collision probability of CE molecules with themselves.

FTIR was employed to study the influence of CRBN on the curing behavior of CE at 170 °C. The reaction during cure process was tracked mainly by paying attention to the –C≡N stretching band at 2272 cm^{-1} as the cyanate group of CE resin. As shown in Fig. 3, the intensity of this absorption band decreases during the cure process, and the intensity of the absorption band at 1565 cm^{-1} (–C=N stretching band of polytriazine) increased. The reaction of the CE resin is cyclotrimerization of the cyanate groups to form a highly crosslinked polycyanurate network in the absence or presence of CRBN (Scheme 1 of Fig. 4). As shown in Fig. 3, a new weak absorption band at 2330 cm^{-1} is found during the cure process. And its intensity increases in the first 20 min and did not change anymore afterwards. This absorption band could be attributed to the –N=C=O stretching band. At the beginning of the measurements, the reaction rate of the cyclotrimerization is relatively slow, and the cyanate groups of some CE molecules may have an isomeric change to isocyanate (Scheme 2 of Fig. 4). According to Fig. 3, more isomeric changes occur in the pure CE system than the CE/CRBN system. It refers that the CRBN had an activation effect to CE curing reaction. It is in accordance with the DSC results that the onset temperature of the cure process of CE decreases with the addition of CRBN.

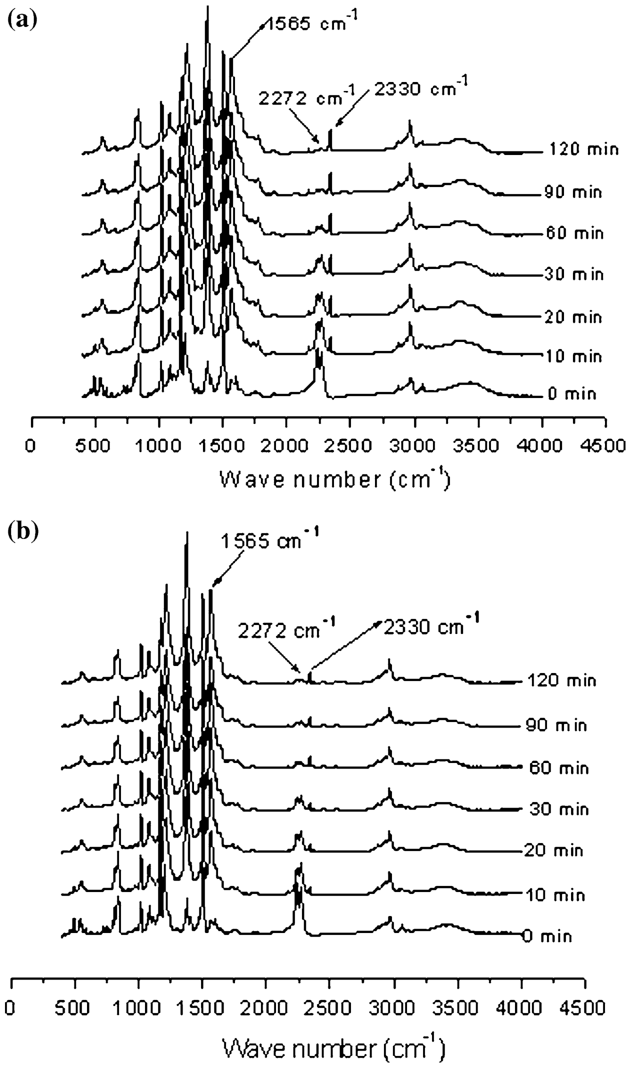

Fig. 3 Curing behavior of pure CE (**a**) and CE/CRBN (CRBN 8%) (**b**) studied by FTIR

Phase behavior of the system

The fracture surface of rubber-modified CE networks was analyzed by SEM (Fig. 5). The pure CE shows a brittle fracture surface. With the addition of CRBN, the composites have much rougher fracture surface. There is an interesting phenomenon in the SEM images of the composites containing different weight percentage of CRBN: no pore is found in the fracture surface of CE/CRBN (CRBN 5%) in Fig. 5b; few pore is found in the fracture surface of CE/CRBN (CRBN 8%) in Fig. 5c; a small quantity of pores are found in the fracture surface of CE/CRBN (CRBN 15%) in Fig. 5d and some cracks are terminated by the pores. With the addition of CRBN, no globular nodules are observed in the samples' fracture surface. This means the pores hardly result from some CRBN particles that pulled out during fracture process. The formation of pores mainly results from a slight weight loss of CRBN during the curing cycle. The gas molecules (the decomposition products of low molecular weight part of CRBN) were trapped by the crosslinking network of CE and formed the pores. It is similar to the reported results of CE/CTBN system [9, 10, 20]. However, both the size and number of the pores in the present study are smaller than in CE/CTBN. As shown in Fig. 6, the main reason is that CRBN used in the present study has a higher thermal stability during the curing cycle than CTBN used in the recent work [20].

In order to view phase separated rubber particles with TEM, the ultra thin sample films were treated firstly by osmium tetraoxide (OsO_4). The unreacted C=C within the rubber phase could be dyed and the rubber phase exhibited a dark zone in the TEM photos. As shown in Fig. 7, neat CE shows no special feature and CE/CRBN is still a phase separation system. The black globular content observed in Fig. 7b is CRBN-rich phase. The dispersed rubber phase size of CE/CRBN (CRBN 8%) is 0.1–1 μm. In addition, there are also some white globular content observed in Fig. 7b. This is assigned to the pores

Fig. 4 Scheme of the cure and isomeric change of CE

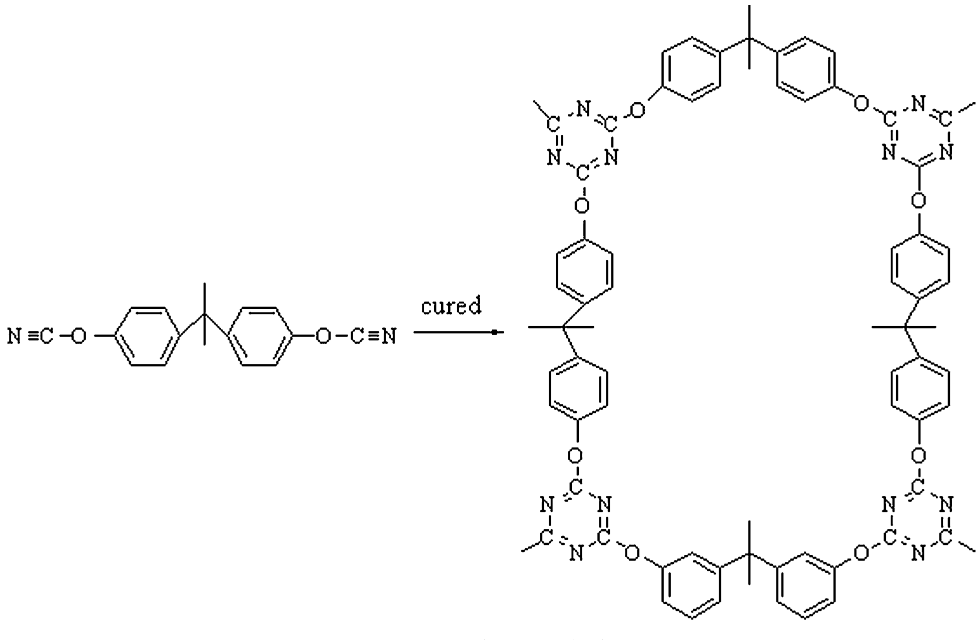

1. Cure scheme of CE.

$$R-O-C\equiv N \longrightarrow R-N=C=O$$

2. Isomeric change of CE.

Fig. 5 SEM images of the fractured surface of pure CE and CE/CRBN composites: **a** pure CE; **b** CRBN (5%); **c** CRBN (8%); **d** CRBN (15%)

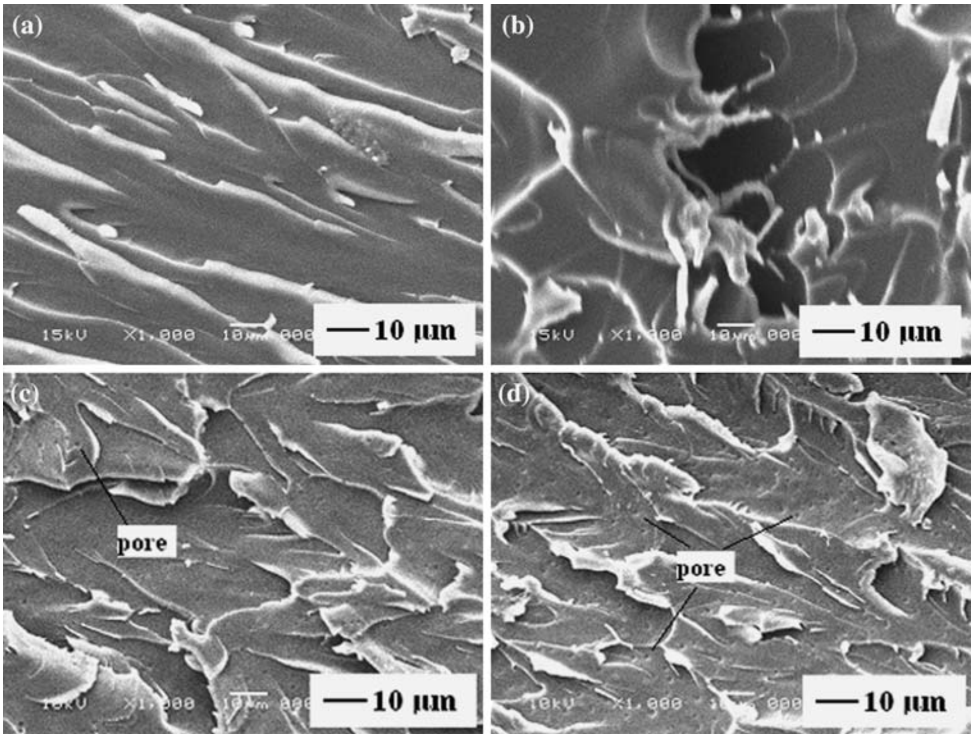

containing in the samples. These results verified that CE/CRBN is a multi-phase system containing some pores. Such phase behavior of the composite can be summarized in Fig. 8.

Free-volume properties of the system

The PALS spectra for all samples were analyzed with PATFIT for three or more components of lifetime. For all

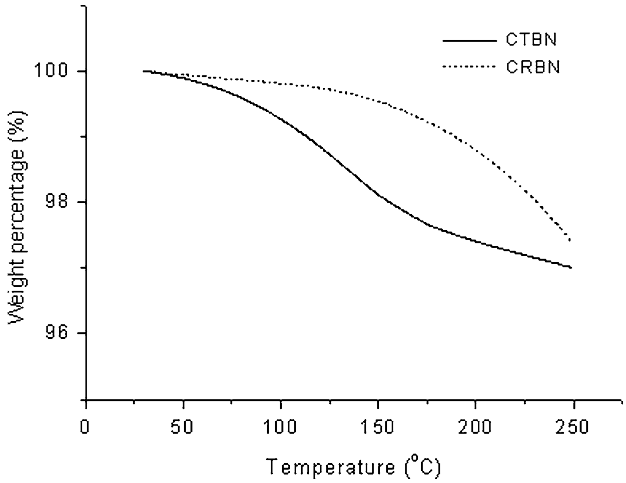

Fig. 6 Weight percentage as a function of temperature for pure CTBN and CRBN under nitrogen atmosphere

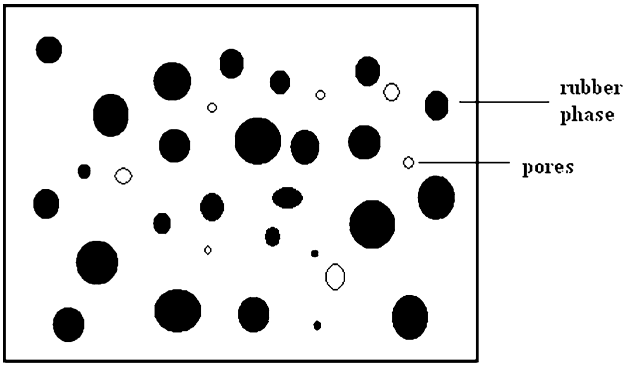

Fig. 8 Schematic phase behavior of the composite

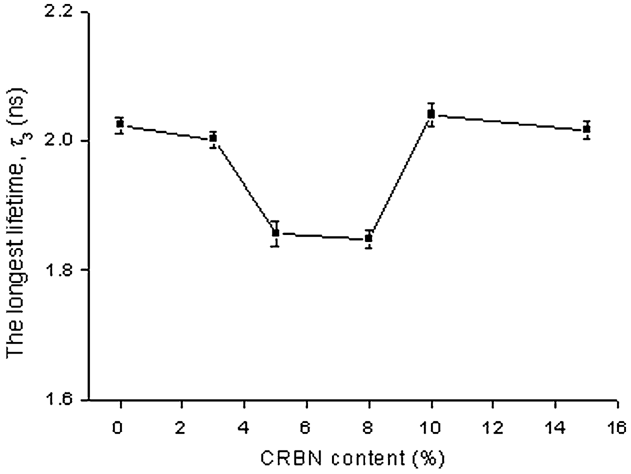

Fig. 9 The longest lifetime τ_3 of the composites with different CRBN content

samples a three-component fit was much better with variances all below a value of 1.2. Usually, the shortest lifetime τ_1 is attributed to *p*-Ps annihilation. The intermediate lifetime τ_2, is from the free positron annihilation. The longest lifetime τ_3, is assigned to *o*-Ps annihilation. The CRBN content dependence of the *o*-Ps lifetime τ_3, its intensity I_3, and the intensity of the intermediate lifetime I_2 are shown in Figs. 9 and 10. According to the SEM observation, if the CRBN content was low ($\leq$8%), there are almost no pores induced. The influences of the induced pores on the positron annihilation parameters could be neglected. As shown in Figs. 9 and 10, when the CRBN content is low ($\leq$8%), the *o*-Ps lifetime τ_3 of the composite decreases as the CRBN content increases. Its intensity I_3 also decreases as the CRBN content increases. The intensity of the intermediate lifetime I_2 shows an increase as the CRBN content increases.

These changes in positron annihilation parameters can be explained as follows. Previous studies [23, 24] had showed that in the case of thermosetting-based composites, chains are restricted in the rigid network structure (in which chain units connect with chemical bond) and their mobility depends much more on the properties of the

Fig. 7 TEM image of CE (**a**) and CE/CRBN (CRBN 8%) (**b**)

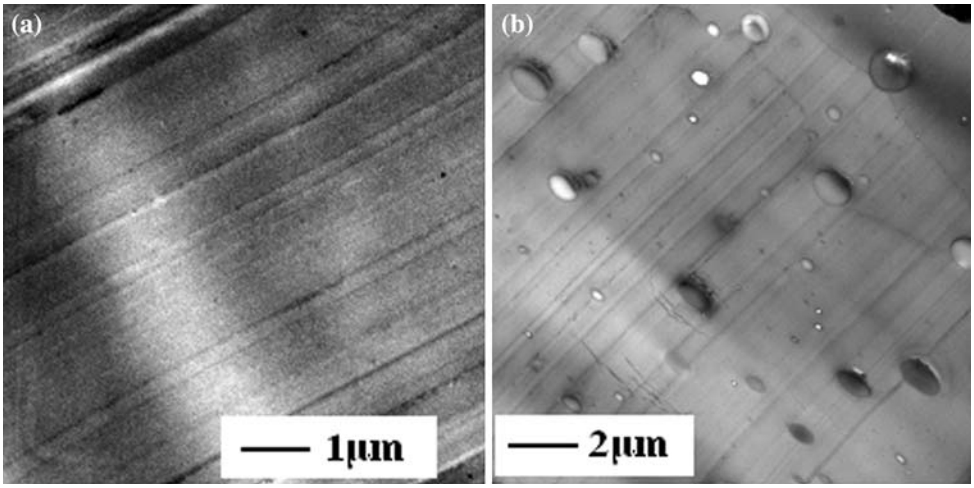

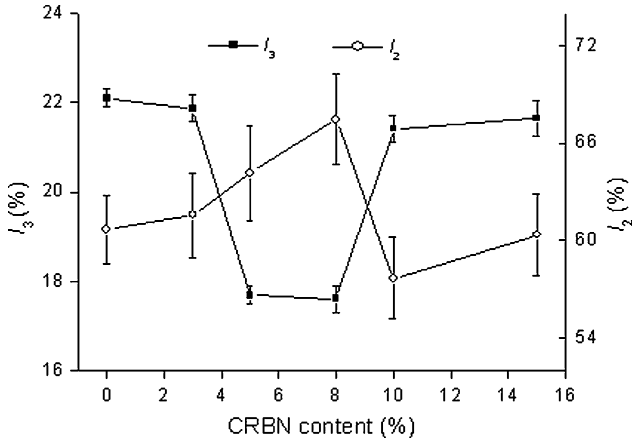

Fig. 10 The intensity of the intermediate lifetime component I_2, the intensity of the longest lifetime component I_3 of the composites with different CRBN content

network, such as chemical structure and crosslinking density. The size and concentration of free-volume holes are mainly determined by the backbone structure, which depends strongly on the conversion of cure reaction. According to Eq. 1, the average radius R of the free-volume holes of pure CE matrix can be calculated and its value is 0.2870 nm [20]. All the specimens that were modified with CRBN with different weight percentage have lower free-volume concentration than pure CE. On the one hand, the size of CRBN phase that separated from the CE matrix is in micrometer level. It is hard to enter the free-volume hole of CE matrix owing to its size. Thus, the separated CRBN particles could occupy a number of free-volume holes of the CE matrix and inducing a deformation of the network. This would lead to a decrease in the total free-volume concentration of the composites. On the other hand, the interaction between the matrix and filled-in rubber particles could restrict the segmental chain motion, leading to a decrease in the free-volume concentration. Therefore, I_3 decreases as the CRBN is added. For a polymer base composite filled with particles, a correlation is that the interfacial property of the composites can be reflected in the intensity of the intermediate lifetime component I_2 [23–26]. For the rubber content from 0 to 8%, an increase of I_2 is observed from Fig. 10. This might be related to the strong interfacial adhesion between the CRBN particles and CE matrix. In the interfacial zone, all kinds of interfacial interactions between CE matrix and CRBN particles come from the interactions of polar groups of CRBN and CE molecules. The concentrate of polar groups might be higher in interfacial zone. The polar groups are often electro-attracting for its high electronegativity and act as electron scavengers and positron capturers [27]. Therefore, the intermediate lifetime component comes from not only the free positron annihilation in the body state of the polymers, but also polar groups trapping positrons in the interfacial layers for its strong interfacial adhesion. When the rubber content is low, rubber particles are relatively small and dispersed uniformly in the CE matrix. The amount of interfacial layers should increase with increasing rubber content.

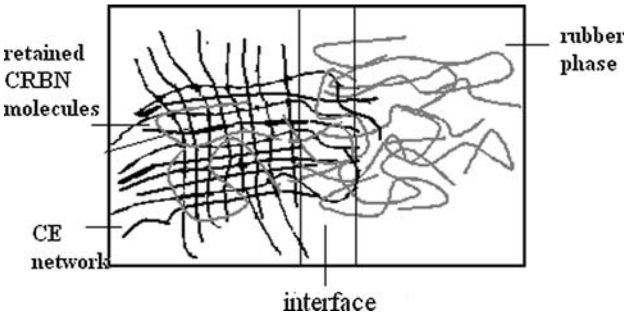

Fig. 11 Fine phase morphologies of the composites

As seen from the SEM and TEM images, the blend system is still a phase separation system though there are a fairly well interfacial adhesion and compatibility between the blend components. During the polymerization, the rubber phase separates because it becomes less miscible with the matrix and forms tiny particles of rubber that are dispersed in the matrix. The rubber phase is more preciously a rubber-rich phase that retained some CE molecules. Similarly, the CE matrix is a CE-rich phase that retained some CRBN molecules (as shown in Fig. 11). Within the CE-rich phase, the retained CRBN chains could enter the free-volume holes of CE matrix because the functional groups of CRBN chains were capable to react with CE, leading to a partition effect to the free-volume hole of the CE-rich phase. Such partition effect would lead to a decrease in the free-volume size of CE matrix. This may be the factor determining the decrease in *o*-Ps lifetime τ_3 of the composite.

If the CRBN content is high ($\geq$10%), the changes in positron annihilation parameter of the composite might be more complicated. The main reason is that the positron annihilation process in the induced pores region would have remarkable influences on the positron annihilation parameters of the composite. As seen from Figs. 9 and 10, the main changes in positron annihilation parameter of the composite are: longer *o*-Ps lifetime τ_3 and higher I_3 in cases of high rubber content is found; I_2 in cases of high rubber content is much lower. In the present study, the induced pores are not empty but filled with gas molecules. When the e^+ was injected into such pores, there is a high probability that the positron will become bound to an electron from a gas molecule before it is finally annihilated. If the positron does not become bound to an electron from a gas molecule, then it will eventually be annihilated, in its free state. The positron/positronium annihilation with electrons of the filled gas molecular must be reasonable. Some of these positrons will annihilate as free positrons and some will form additional Ps [28, 29]. Our recent study [20] showed that there might be a competition between the Ps formation and the gas molecules trapping positron in the induced pores. The higher I_3 should be much related to the contribution of the additional Ps annihilation in the induced pores. The *o*-Ps annihilation lifetime in the induced pores is reasonably longer than in the free-volume hole of the polymers. In addition, the contribution of *o*-Ps annihilation in the rubber phase to the lifetime component τ_3 of the composite could not be neglected anymore when the rubber content is high. Generally, the rubber phase is much looser than the crosslinked CE matrix because of its amorphous structure. The size of the free-volume holes within the rubber phase is larger than in the CE network, resulting in an increasing effect on the mean free-volume size of the composites. Thus, both the τ_3 and its intensity I_3 are relatively higher in the cases containing high rubber content. Two aspects can explain the reason of the lower I_2. On the one hand, more Ps form and then the free positron annihilation decreases. On the other hand, when the rubber content is high, rubber tends to form big particles and cannot disperse uniformly in the CE matrix. The interfacial area and the interfacial interaction between the rubber phase and the CE matrix decrease.

Toughening behavior and mechanism

The impact strength of CE/CRBN composites were measured and shown in Fig. 12. A significant increase in the impact strength of all the samples added with CRBN, when compared to that of unfilled CE is observed. CRBN has a much better toughness modification effect to CE matrix than CTBN used in recent works [9, 10, 20]. It is mainly attributed to the stronger interfacial adhesion and higher thermal stability of the used CRBN. Meanwhile, the compatibility and interfacial adhesion of the composites can be inferred from the changes in free-volume properties of the composites.

The impact behavior of the toughened CE networks could be explained by considering both toughening and flexibilizing effects [30, 31]. The flexibilizing effect is caused by the presence of dissolved rubber inside CE matrix. The toughening effects are related to the cavitations in rubber particles dispersed inside the CE matrix. The rubber particles initiate the formation of crazes and control their growth. The toughening effects are determined by the rubber particles size and the interfacial interaction between the rubber particles and the CE matrix. Both of these two effects are consistent with the PALS results. As seen from Fig. 9, the mean free-volume size of the system decreases first up to 8% CRBN, and then increases with further addition of CRBN. The first decrease in the mean free-volume size of the system is mainly related to the partition effects of the dissolved CRBN molecules to the free-volume holes of CE matrix, indicating fairly well interfacial adhesion and compatibility between the blend components. Good interfacial adhesion is also reflected by the higher I_2 of the composite. Such well interfacial adhesion and compatibility are necessary for efficient stress transfer between the rubber particles and CE matrix. Therefore, the toughness of the composite increases as CRBN is added. With further addition of CRBN to CE, CRBN tends to form big particles and the interfacial adhesion between the rubber phase and CE matrix then decreases. As discussed above, a reduction of the interfacial interaction would lead to an increase in the mean free-volume size of the composites. In addition, PALS is

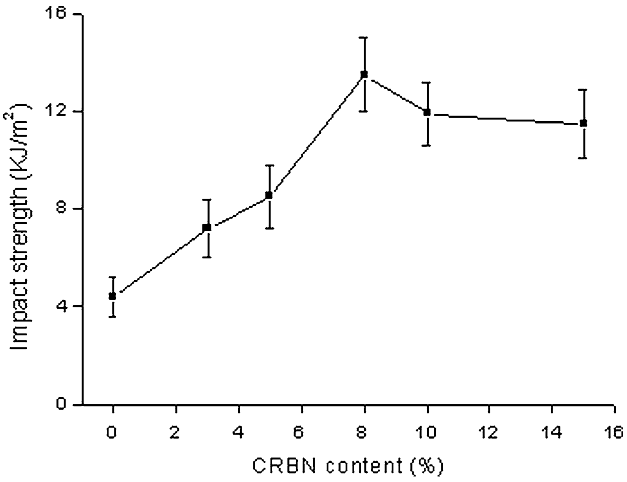

Fig. 12 The impact strength of the composites with different CRBN content

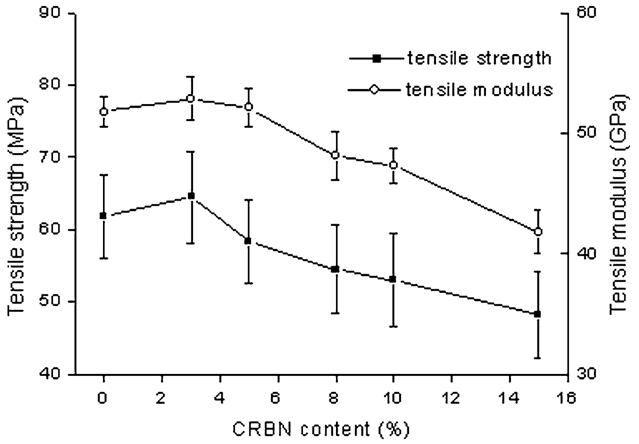

Fig. 13 The tensile properties of the composites with different CRBN content

qualitatively sensitive to the existence of pores induced by low molecular weight part of CRBN during curing process. The induced pores might be another toughening mechanism that ever proposed by several investigators [32, 33]. The decrease in the tensile strength and modulus (as shown in Fig. 13) of the composites is mainly attributed to the lower modulus of the rubber component.

Conclusions

The toughness of CE matrix is improved significantly with addition of CRBN. Phase separation is the main toughening mechanism for CE/CRBN composites. The existence of micro-pores induced by low molecular weight part of CRBN during curing process is another toughening mechanism. For comparing, CRBN has a better toughness modification effect to CE matrix than CTBN used in other works. The toughening mechanism is proved powerfully from the aspect of free-volume using PALS.

Acknowledgements This work is supported by National Nature Science Foundation of China (Grant number 10875079), and Nature Science Foundation of Zhejiang Province, China (Grant number Y4080448).

References

1. McGarry FJ (1996) In: Arends CB (ed) Polymer toughening. Marcel Dekker, New York, p 175
2. Huang Y, Hunston DL, Kinloch AJ, Keith RC (1993) Rubber toughened plastics, ACS advances in chemistry series 233. American Chemical Society, Washington, DC, p 1
3. Hayes BS, Seferis JC (2001) Int SAMP Symp Exhib 46:1072
4. Hayes BS, Seferis JC, Parker GA (2000) Polym Eng Sci 40:1344
5. Borrajo J, Riccardi CC, Williams RJJ, Cao ZQ, Pascault JP (1995) Polymer 36:3541
6. Wang JL, Liang GZ, Zhao W, Lu SH, Yan HX (2006) Polym Eng Sci 46:581
7. Hillermerier RW, Hayes BS, Seferis JC (1999) Polym Compos 20:155
8. Cao Z, Mechin F, Pascault JP (1994) Polym Int 34:41
9. Feng Y, Fang ZP, Gu AJ (2004) Polym Adv Technol 15:628
10. Feng Y, Fang ZP, Gu AJ (1994) Polym Int 54:369
11. Shi HH, Fang ZP, Gu AJ, Tong LF, Xu ZB (2007) J Appl Polym Sci 106:3098
12. Ito K, Kobayashi Y (2003) Appl Phys Lett 82:654
13. Hu YH, Qi CZ, Liu WM, Wang BY, Sun XD, Zheng HT (2003) J Appl Polym Sci 90:1507
14. Jean YC (1990) Microchem J 42:72
15. Pethrick Richard A (1997) Prog Polym Sci 22:1
16. Tao SJ (1972) J Chem Phys 56(12):5499
17. Nakanishi H, Wang SJ, Jean YC (1988) In: Sharma SC (ed) Positron annihilation in fluids. World Sci. Pub., Singapore, p 292
18. Zeng MF, Sun XD, Xiao HQ, Ji GZ, Jiang XW, Wang BY, Qi CZ (2008) Radiat Phys Chem 77:245
19. Zeng MF, Sun XD, Yao XD, Ji GZ, Chen N, Wang BY, Qi CZ (2007) J Appl Polym Sci 106:1347
20. Zeng MF, Sun XD, Wang Y, Zhang MZ, Shen YM, Wang BY, Qi CZ (2008) Polym Adv Technol 19:1664
21. Shimp DA, Hudock FA, Ising SJ (1988) Int SAMPE Symp Exhib 33:754
22. Gupta AM, Macosko CW (1991) Makromol Chem, Macromol Symp 45:105
23. Yu DH, Wang B, Feng Y, Fang ZP (2006) J Appl Polym Sci 102:1509
24. Liu LM, Fang PF, Zhang SP, Wang SJ (2005) Mater Chem Phys 92:361
25. Zhang M, Fang PF, Zhang SP, Wang B, Wang SJ (2003) Radiat Phys Chem 68:565
26. Wang B, Qi N, Gong W, Li XW, Zhen YP (2007) Radiat Phys Chem 76:146
27. Qi CZ, Wang W, Wu YJ, Zhang SH, Wang HJ, Li HM, Wang TM, Yan FY (2000) J Polym Sci B: Polym Phys 38:435
28. Wilkinson NJ, Duffy JA, Fretwell HM, Alam MA (1995) Phys Lett A 204:285
29. Duffy JA, Alam MA (2000) Langmuir 16:9513
30. Fabio LB, Thiago PA, Bluma GS (2003) Polymer 44:5811
31. Bucknall CB (1977) Toughened plastics. Applied Science Publishers, London, p 188
32. Bagheri R, Pearson RA (1996) Polymer 37:4529
33. Bagheri R, Pearson RA (1995) Polymer 36:4883